RSC Advances

PAPER

View Article Online
View Journal | View Issue

Cite this: *RSC Adv.*, 2021, **11**, 33186

Origin of photoluminescence of water-soluble $CuInS_2$ quantum dots prepared *via* a hydrothermal method†

Kazutaka Iida, Yota Uehigashi and DaeGwi Kim *

This study was performed to investigate the origin of the photoluminescence (PL) properties of hydrothermally-synthesized water-soluble $CuInS_2$ (CIS) quantum dots (QDs). The corresponding PL decay profiles, time-resolved PL spectra, and excitation intensity dependence of the PL spectra were evaluated. The decay profiles exhibited a strong dependence on the detection energy, and the peak of the time-resolved PL spectra shifted to lower energies with increasing time. With increasing excitation light intensity, the PL peak shifted to the high-energy side. These experimental results were consistent with the characteristics of donor–acceptor pair emission. The PL properties of Cu-doped and non-doped CdSe QDs, which show Cu-related and defect-related PL emission, respectively, were compared. Based on these results, it was concluded that donor–acceptor pair emission is the underlying mechanism of the PL of the hydrothermally-synthesized water-soluble CIS QDs.

Received 29th July 2021
Accepted 1st October 2021

DOI: 10.1039/d1ra05761h

rsc.li/rsc-advances

Introduction

Owing to their size, semiconductor quantum dots (QDs) exhibit optical properties different from those exhibited by bulk crystals because the electrons and excitons are under the influence of three-dimensional confinement.[1–5] The intrinsic energy of QDs can be controlled by changing their size, and their photoluminescence (PL) efficiency is very high.[6–9] Owing to these characteristics, QDs have garnered widespread attention in recent years and have been actively studied for applications in displays, light-emitting diodes (LEDs),[10] bioimaging,[11] and solar cells.[12] To date, the reported studies on QD have been primarily focused on Cd-based QDs, which exhibit high PL quantum yields (PLQYs).[13–16] However, in recent times, environmental load reduction has moved under the spotlight as a necessary step for environmental sustainability. Numerous worldwide efforts are being made in this direction in all the fields of science and technology, and as a result of such efforts, $CuInS_2$ (CIS) QD has emerged as a viable alternative to Cd-based QD. CIS is a direct transition semiconductor with a bandgap energy of 1.53 eV and absorption and PL wavelengths in the near-infrared region. Therefore, CIS QDs are expected to become the next-generation materials for solar cells, LEDs, display devices, and bioimaging applications.[17–19]

Although a series of studies have been conducted on CIS QDs, in most of them, a hot-injection method has been employed for the QD synthesis.[20–30] However, the hot-injection synthesized QDs are oil soluble and hence are not suitable for bioimaging applications. Therefore, in our previous study, we directly synthesized water-soluble CIS QDs and CIS/ZnS core/shell QDs using the hydrothermal method.[31,32] We optimized the synthesis conditions such as the Cu:In:S ratio, reaction temperature, and reaction time and successfully fabricated CIS QDs exhibiting a PLQY of 4%. Furthermore, an increase of 30% was observed in the PLQY of the synthesized CIS/ZnS core/shell QDs.[32]

Majority of the previously reported studies on CIS QDs revolved around the synthesis of CIS QDs with high PL efficiency; however, recently, several studies have been performed to investigate the origin of the PL of CIS QDs. Zhong *et al.* reported that the PL characteristics of CIS QDs originates from "donor–acceptor pair" (DAP) emission, based on experimental time-resolved PL spectroscopy and PL decay profile results.[33] Furthermore, Li *et al.* experimentally measured the PL spectra, PL decay profiles, and transient absorption spectra of CIS QDs and reported that their PL characteristics are caused by the internal and surface defects.[34]

However, recently, Knowles *et al.* conducted detailed experiments comparing the absorption spectra, PL spectra, PL decay profiles, and magnetic circularly polarized PL properties of two types of Cu-doped samples, namely Cu:CdSe and Cu:InP, as well as of CIS QDs.[35] Based on the similar PL spectra along with the magnitude of the Stokes shift and magnetic exchange splitting energy of the singlet and triplet excited states for these three types of QDs, they reported that the origin of the PL properties of CIS QDs was same as that of the Cu-doped semiconductor QDs with Cu^+ sites containing highly localized holes. Rice *et al.* also reported that the PL characteristics of CIS QDs arise from a Cu-related PL band. This result was established by comparing the experimentally

Department of Applied Physics, Graduate School of Engineering, Osaka City University, 3-3-138, Sugimoto, Sumiyoshi-ku, Osaka 558-8585, Japan. E-mail: tegi@a-phys.eng.osaka-cu.ac.jp

† Electronic supplementary information (ESI) available. See DOI: 10.1039/d1ra05761h

obtained absorption spectra, magneto PL properties, and magnetic circular dichroism of three types of QDs, namely, CIS, Cu:ZnSe, and CdSe.[36] However, all these studies were primarily centered on identifying the origin of the PL characteristics of oil-soluble CIS QDs synthesized using a hot-injection approach.

In contrast, the studies on water-soluble CIS QDs were mostly focused on the fabrication of CIS QDs.[37–40] To date, only a few studies have been conducted to evaluate the origin of the PL properties of water-soluble CIS QDs. In this paper, we report the results of a detailed investigation on identifying the origin of the PL properties of water-soluble CIS QDs, which were prepared using the hydrothermal method. Typically, such experiments need to be conducted at cryogenic temperatures to neglect the effect of non-radiative recombination processes. In this study, we fabricated film samples in which CIS QDs were uniformly dispersed and measured their PL characteristics such as PL decay profiles, time-resolved PL spectra, and the excitation intensity dependence of the PL spectra at a low temperature of 15 K. We compared the experimental results of CIS QDs with those of Cu^{+}-doped Cu:CdSe/ZnS QDs, which exhibit Cu-related PL emission, and non-doped CdSe QDs, which show defect-related PL emission. These results showed that the PL characteristics of the water-soluble CIS QDs originates from the DAP emission.

Experimental section

In this study, CIS QDs were prepared using hydrothermal method following the procedure described in ref. 32. First, a precursor solution was prepared by mixing $CuCl_2 \cdot 2H_2O$, $InCl_3 \cdot 4H_2O$, and $Na_2S \cdot 9H_2O$ as the Cu, In, and S ion sources, respectively, with the ligand *N*-acetyl-L-cysteine (NAC) in ultrapure water as a solvent with a molar ratio of 1 : 2 : 2.4 : 18. Subsequently, this precursor solution was heated in an autoclave at 180 °C for 30 min to prepare the CIS QDs. We confirmed the successful fabrication of CIS QDs, each with a diameter of 5.4 nm and chalcopyrite structure, *via* transmission electron microscopy and X-ray diffraction measurements.[32] Next, we dispersed the colloidal CIS QDs into pullulan films using the following procedure to study their PL properties at low temperatures: initially, two aqueous solutions of CIS QDs and pullulan were mixed; the resulting solutions were then spread on a glass substrate and subsequently heated at 80 °C for 2 h to evaporate the excess water.

The absorption spectra were measured using a double beam spectrophotometer (JASCO V-650) with a resolution of 0.2 nm. The PL spectra and decay profiles were acquired using an SHG:YAG laser (532 nm) (CryLas GmbH, FDSS532-Q2), with a pulse duration of 1.5 ns and a repetition frequency of 10 kHz, as the excitation source. The emission from the sample was analyzed using a single monochromator (Jobin-Yvon HR-320) with a resolution of 1 nm. The excitation light intensity was adjusted using neutral density filters, and the PL decay profiles were obtained using the time-correlated single-photon counting method.

Results and discussion

The absorption spectra, PL spectra, and PL decay profiles of the colloidal solution and film samples of the synthesized CIS QDs at room temperature are shown in Fig. S1.† The PL decay profiles were measured by detecting the PL intensity at the PL peak energy of 1.66 eV. The experimental results for both the samples were consistent, showing that the CIS QDs were dispersed in the film while preserving the optical properties of the solution. To investigate the origin of the PL in the CIS QDs, measuring the PL properties at cryogenic temperatures is crucial for suppressing the nonradiative recombination processes; thus, the PL properties of the synthesized CIS QDs were examined in detail at a low temperature of 15 K using the fabricated film samples in which the CIS QDs were uniformly dispersed.

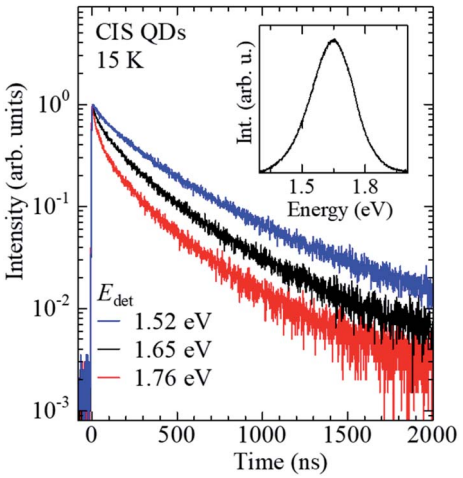

Fig. 1 PL decay profiles of CIS QDs at 15 K, detected at the PL peak energy (1.65 eV) as well as at energies that are higher (1.76 eV) and lower (1.52 eV) than that of the peak energy. The inset shows the PL spectrum at 15 K.

Fig. 1 shows the PL decay profiles of the CIS QDs at 15 K, detected at the PL peak energy (1.65 eV) as well as at energies that are higher (1.76 eV) and lower (1.52 eV) than that of the peak energy. These two off-peak energies correspond to the energies at which the intensities become half of the peak intensity. The inset shows the PL spectrum at 15 K. Evidently, the PL decay exhibits a long decay profile of the order of microseconds and is strongly dependent on the detection energy. Fig. 2 shows a time-resolved PL color map of the CIS

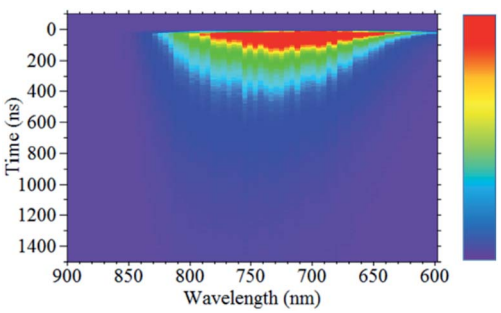

Fig. 2 Time-resolved PL color map of CIS QDs at 15 K, which was obtained by three-dimensionally plotting PL decay profiles measured using different detection wavelengths in the range of 600–940 nm with an increment of 5 nm.

QDs at 15 K, obtained by three-dimensional plotting of the PL decay profiles measured using different detection wavelengths in the range of 600–940 nm with an increment of 5 nm. The delay time dependence of the time-resolved PL spectra and the PL peak energy are shown in Fig. 3. Evidently, the peak in the time-resolved PL spectra shifts to lower energies with increasing delay time, reflecting that the PL at higher energies involves a higher radiative recombination rate and decays in a shorter time. These experimental results suggest that the PL emitted by the hydrothermally-synthesized water-soluble CIS QDs originates from DAP emission.

The DAP emission results from the recombination of electrons trapped at the donor level and holes trapped at the acceptor level, and the corresponding PL energy (E_{PL}) can be expressed using the following equation:[41–43]

$$E_{PL} = E_g - (E_D + E_A) + e^2/4\pi\varepsilon r \quad (1)$$

where E_g is the band gap energy; E_D and E_A are the binding energies of the donor and acceptor, respectively; r is the distance between the donor and acceptor; and ε is the dielectric constant. As shown in eqn (1), the DAP recombination is characterized by the PL energy changes due to the Coulomb interaction between the donor and acceptor. Therefore, when the distance between the donor and the acceptor decreases, the PL energies increase and *vice versa*. Moreover, a smaller distance between the electron at donor level and the hole at acceptor level results in a larger overlapping of their respective wavefunctions, which in turn leads to a higher oscillator strength, and the radiative recombination rate increases. Therefore, for the PL originating from DAP emission, a higher PL energy corresponds to a shorter PL decay time. The experimental results shown in Fig. 1 and 3 are consistent with the features of DAP emission.

Fig. S2,† shows the excitation intensity dependence of the CIS QD PL spectra at 15 K. Fig. 4a shows the enlarged PL spectra near the PL peak, where the downward arrows indicate the PL peak energy estimated from the minimum point of the second-derivative PL spectra. The dependence of the PL peak energy on the excitation intensity is depicted in Fig. 4b, which shows that the PL peak shifts to higher energies with increasing excitation intensity. The low-energy component of the DAP emission corresponds to the donor–acceptor pair with a large distance between them, and a larger donor–acceptor distance results in a smaller oscillator strength. Consequently, with increasing excitation intensity, the intensity of the higher energy component, which is associated with a larger oscillator strength, increases because the lower energy component is more likely to cause saturation of the state. This implies that as the excitation intensity increases, the DAP emission peak shifts to a higher energy. From these experimental results of the photodetection energy dependence of the PL decay profiles and the excitation intensity dependence of the PL spectra, it can be concluded that the DAP emission is the origin of the PL of water-soluble CIS QDs.

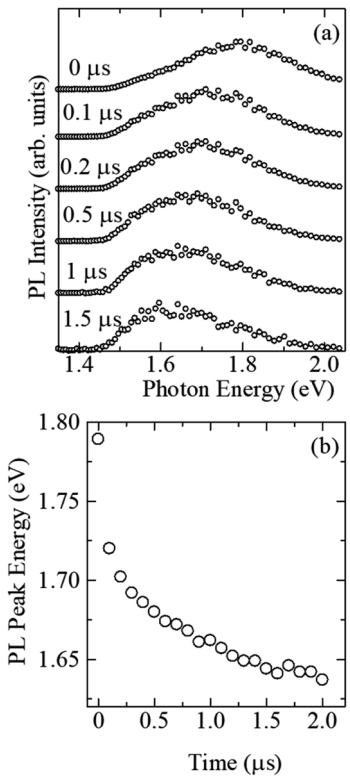

Fig. 3 (a) The delay time dependence of the time-resolved PL spectra of CIS QDs at 15 K. (b) The dependence of the PL peak energy on the delay time.

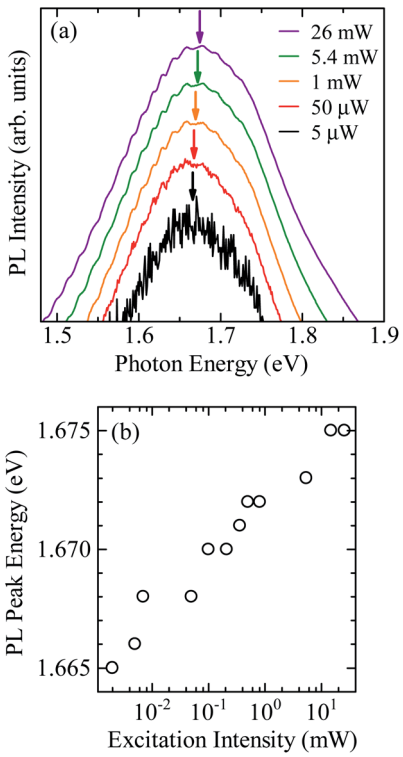

Fig. 4 (a) Excitation intensity dependence of the enlarged PL spectra near the PL peak of CIS QDs at 15 K. The downward arrows indicate the PL peak energy estimated from the minimum point of the second-derivative PL spectra. (b) The dependence of the PL peak energy on the excitation intensity.

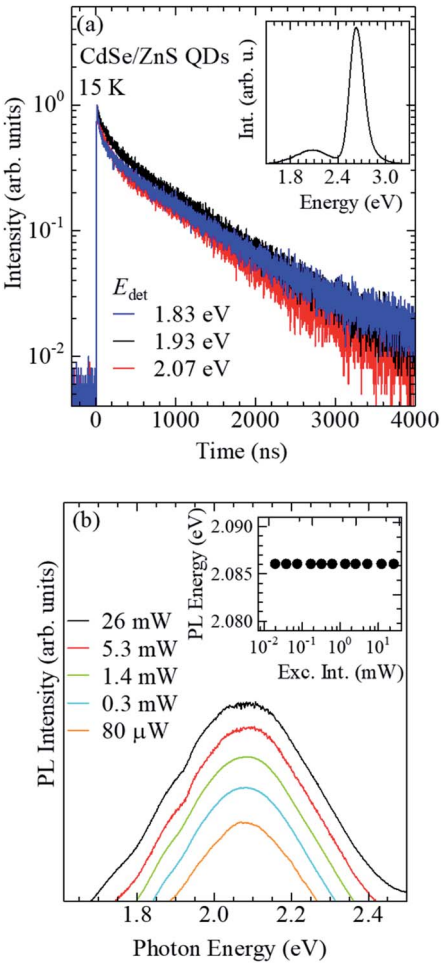

Fig. 5 (a) PL decay profiles, detected at 1.83, 1.93, and 2.07 eV, in the CdSe/ZnS QDs at a temperature of 15 K. The PL spectrum is shown in the inset. (b) Excitation intensity dependence of PL spectra expanded in the vicinity of the peak of the defect-related PL band. The inset shows the dependence of the PL peak energy on the excitation intensity.

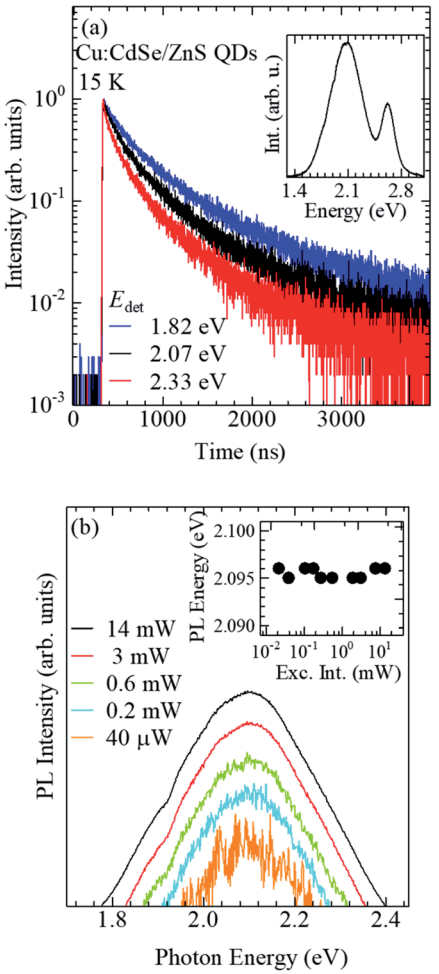

Fig. 6 (a) PL decay profiles, detected at 1.82, 2.07, and 2.33 eV, for the Cu:CdSe/ZnS at a temperature of 15 K. The PL spectrum is shown in the inset. (b) Excitation intensity dependence of PL spectra expanded in the vicinity of the peak of the Cu-PL band. The inset shows the dependence of the PL peak energy on the excitation intensity.

However, recently, Knowles *et al.* compared the PL properties of CIS QDs with those of Cu-doped Cu:CdSe and Cu:InP QDs and reported that the origin of the PL of the CIS QDs was Cu-related, *i.e.*, mediated by Cu ions. Notably, these QDs were oil-soluble and synthesized using the hot-injection method with oleic acid as the ligand.[35] In the study reported in ref. 34, 1-dodecanethiol was used as the solvent, S source, and ligand. In contrast, in the present study, the precursor solution was prepared by mixing NAC as the ligand and Na_2S as the S source with Cu and In ion sources. Therefore, the formation mechanism of the oil-soluble and water-soluble CIS QDs might be different. Furthermore, the ligand sources, oleic acid for the oil-soluble QDs reported in ref. 35 and NAC for the water-soluble QDs prepared in this study, were completely different, indicating the possibility that the origin of PL of these QDs is different.

Therefore, to assess whether Cu-mediated PL can be the origin of the PL of the water-soluble CIS QDs, we hydrothermally synthesized water-soluble Cu:CdSe/ZnS QDs as well and investigated the photodetection energy dependence of the PL decay profiles and the excitation intensity dependence of the PL spectra. In addition, we investigated the possibility of defect-related PL by synthesizing water-soluble CdSe/ZnS QDs and performing similar experiments that were focused on evaluating the defect-related PL characteristics of these QDs.

Here, we first discuss the PL properties of the CdSe/ZnS QDs. Fig. 5a shows PL decay profiles, detected at 1.83, 1.93, and 2.07 eV, in the CdSe/ZnS QDs at a temperature of 15 K; the PL spectrum is shown in the inset. The main PL band on the high energy side corresponds to band-edge PL and that on the low energy side originated from defect-related PL, which was the focus of this study. Noticeably, the decay profiles of the defect-related PL are independent of the detected energy. Fig. 5b shows the excitation intensity dependence of PL spectra of the CdSe/ZnS QDs at 15 K; these spectra are expanded in the vicinity of the peak of the defect-related PL band. In addition, the excitation intensity dependence of the PL peak energy is shown in the inset. The peak energy of the defect-related PL in the CdSe/ZnS

QDs does not change with increasing excitation intensity. The results of the detection energy dependence of the decay profiles and the excitation intensity dependence of the spectra of the defect-related PL of the CdSe/ZnS QDs are completely different from those of the PL shown by the CIS QDs (Fig. 1 and 4). Therefore, the possibility of defect-related PL as the origin of luminescence in CIS QDs can be ruled out.

Next, we discuss the PL properties of the Cu:CdSe/ZnS QDs. Fig. 6a shows PL decay profiles, detected at 1.82, 2.07, and 2.33 eV, for the Cu:CdSe/ZnS at a temperature of 15 K; the inset shows the PL spectrum at 15 K. The main band on the low energy side of the band-edge PL originates from Cu-related PL. We focused our investigation on their Cu-related PL properties. Similar to the results obtained for the CIS QDs, the PL decay profiles of the Cu-related PL band depended on the detection energy, and the profiles became shorter as the detection energy increased. Fig. 6b shows the excitation intensity dependence of the PL spectra of Cu:CdSe/ZnS QDs at 15 K; the spectra are expanded in the vicinity of the peak of the Cu-PL band. Notably, the excitation intensity dependence of the PL spectra of oil-soluble CIS QDs has not yet been reported. Similar to the features of the defect-related PL of CdSe/ZnS QDs, the PL peak energy in this case also does not shift with increasing excitation intensity (Fig. 6b, inset). This result is in stark contrast to those of the CIS QDs, shown in Fig. 4. Thus, although the detection energy dependence of the PL decay profiles of the CIS QDs and Cu:CdSe/ZnS QDs showed similar behavior, a clear difference was observed in the excitation intensity dependence of their PL spectra. Based on these results, the possibility of Cu-related PL being the origin of the PL of the water-soluble CIS QDs can be ruled out as well, and we conclude that DAP emission is the origin of the PL characteristics of the hydrothermally-prepared water-soluble CIS QDs.

Conclusions

To elucidate the origin of the PL emission exhibited by hydrothermally-prepared water-soluble CIS QDs, their PL properties were investigated in detail at a cryogenic temperature of 15 K, where the effects of nonradiative recombination processes can be neglected. The PL decay profiles were dependent on the photodetection energy, and shorter decay profiles were obtained at higher detection energies. Further, the peak in the time-resolved PL spectra shifted to the low-energy side with increasing time. However, a higher excitation intensity caused the PL peak to shift toward the higher energy side. These experimental results are consistent with the characteristics of DAP emission; that is, a smaller distance between the donor and acceptor results in a higher PL energy, higher oscillator strength, and shorter PL decay time; in addition, the state saturation is reduced with increasing excitation intensity.

Furthermore, to examine the possibility of defect-related PL, which was previously considered to be the origin of the PL of CIS QDs, and the possibility of Cu-related PL, which has been proposed as the PL origin for oil-soluble CIS QDs in recent years, as the possible mechanisms in the water-soluble CIS QDs, water-soluble CdSe/ZnS and Cu:CdSe/ZnS QDs were prepared by the hydrothermal method. The excitation intensity dependence of the PL spectra and the photodetection energy dependence of the PL decay profiles were investigated for these prepared QDs. We observed that the peak energy of the defect-related and Cu-related PL bands did not change, even when the excitation intensity was increased. Thus, defect-related and Cu-related PL mechanisms can be eliminated, and we can conclude that DAP recombination is the origin of the PL characteristics of water-soluble CIS QDs.

Author contributions

K. I. and Y. U. designed the experiment, prepared CIS QDs and QDSLs, acquired and analyzed PL spectra and PL decay profiles. D. K. provided conceptual advice. All authors contributed to the interpretation of the results and preparation of the manuscript.

Conflicts of interest

There are no conflicts to declare.

Acknowledgements

This work was supported partially by a Grant-in-Aid for Scientific Research (B) (No. 24560015 and 20H02549) from the Japan Society for the Promotion of Science.

References

1 L. EBrus, *J. Chem. Phys.*, 1984, **80**, 4403.
2 Y. Kayanuma, *Phys. Rev. B: Condens. Matter Mater. Phys.*, 1988, **38**, 9797.
3 L. Brus, *Appl. Phys. A*, 1991, **53**, 465.
4 Y. Wang and N. Herron, *J. Phys. Chem.*, 1991, **95**, 525.
5 R. Zeng, R. Shen, Y. Zhao, Z. Sun, X. Li, J. Zheng, S. Cao and B. Zou, *Cryst. Eng. Comm.*, 2014, **16**, 3414.
6 D. J. Norris and M. G. Bawendi, *Phys. Rev. B: Condens. Matter Mater. Phys.*, 1996, **53**, 16338.
7 D. J. Norris, A. L. Efros, M. Rosen and M. G. Bawendi, *Phys. Rev. B: Condens. Matter Mater. Phys.*, 1996, **53**, 16347.
8 X. Michalet, F. F. Pinaud, L. A. Bentolila, J. M. Tsay, S. Doose, J. J. Li, G. Sundaresan, A. M. Wu, S. S. Gambhir and S. Weiss, *Science*, 2005, **307**, 538.
9 A. P. Alivisatos, *Science*, 1996, **271**, 933.
10 P. O. Anikeeva, J. E. Halpert, M. G. Bawendi and V. Bulovic, *Nano Lett.*, 2009, **9**, 2532.
11 Y. Zhang, C. Xie, H. Su, J. Liu, S. Pickering, Y. Wang, W. W. Yu, J. Wang, J. Hahm, N. dellas, S. E. Mohney and J. Xu, *Nano Lett.*, 2011, **11**, 329.
12 A. J. Nozik, *Phys. E*, 2002, **14**, 115.
13 C. B. Murray, D. J. Norris and M. G. Bawendi, *J. Am. Chem. Soc.*, 1993, **115**, 8706.
14 H. Bu, H. Kikunaga, K. Shimura, K. Takahashi, T. Taniguchi and D. Kim, *Phys. Chem. Chem. Phys.*, 2013, **15**, 2903.
15 D. Kim, H. Yokota, K. Shimura and M. Nakayama, *Phys. Chem. Chem. Phys.*, 2013, **15**, 21051.

16 R. Zeng, Z. Sun, S. Cao, R. Shen, Z. Liu, Y. Xiong, J. Long, J. Zheng, Y. Zhao, Y. Shena and D. Wang, *RSC Adv.*, 2015, **5**, 1083.
17 L. Li, T. J. Daou, I. Texier, T. T. Kim Chi, N. Q. Liem and P. Reiss, *Chem. Mater.*, 2009, **21**, 2422.
18 D. Deng, Y. Chen, J. Cao, J. Tian, Z. Qian, S. Achilefu and Y. Gu, *Chem. Mater.*, 2012, **24**, 3029.
19 J. Kolny-Olesiak and H. Weller, *ACS Appl. Mater. Interfaces*, 2013, **5**, 12221.
20 R. Xie, M. Rutherford and X. Peng, *J. Am. Chem. Soc.*, 2009, **131**, 5691.
21 H. Kim, J. Y. Han, D. S. Kang, S. W. Kim, D. S. Jang, M. Suh, A. Kirakosyan and D. Y. Jeon, *J. Cryst. Growth*, 2011, **326**, 90.
22 L. Li, T. J. Daou, I. Texier, T. T. Kim Chi, N. Q. Liem and P. Reiss, *Chem. Mater.*, 2009, **21**, 2422.
23 M. Booth, A. P. Brown, S. D. Evans and K. Critchley, *Chem. Mater.*, 2012, **24**, 2064.
24 M. Uehara, K. Watanabe, Y. Tajiri, H. Nakamura and H. Maeda, *J. Chem. Phys.*, 2008, **128**, 134709.
25 M. Oda, T. Miyaoka, S. Yamada and T. Tani, *Phys. Procedia*, 2012, **29**, 18.
26 W. Song and H. Yang, *Chem. Mater.*, 2012, **24**, 1961.
27 H. Zhong, Y. Zhou, M. Ye, Y. He, J. Ye, C. He, C. Yang and Y. Li, *Chem. Mater.*, 2008, **20**, 6435.
28 T. Pons, E. Pic, N. Lequeux, E. Cassett, L. Bezdetnaya, F. Guillemin, F. Marchal and B. Dubertret, *ACS Nano*, 2010, **4**, 2531.
29 X. Li, D. Tu, S. Yu, X. Song, W. Lian, J. Wei, X. Shang, R. Li and X. Chen, *Nano Res.*, 2019, **12**, 1804.
30 H. Li, W. Li, W. Li, M. Chen, R. Snyders, C. Bittencourt and Z. Yuan, *Nano Res.*, 2020, **13**, 583.
31 H. Bu, H. Yokota, K. Shimura, K. Takahashi, T. Taniguchi and D. Kim, *Chem. Lett.*, 2015, **44**, 200.
32 K. Iida, Y. Uehigashi, H. Ichida, H. Bu and D. Kim, *Bull. Chem. Soc. Jpn.*, 2019, **92**, 930.
33 H. Zhong, Z. Bai and B. Zou, *J. Phys. Chem. Lett.*, 2012, **3**, 3167.
34 L. Li, A. Pandey, D. J. Werder, B. P. Khanal, J. M. Pietryga and V. I. Klimov, *J. Am. Chem. Soc.*, 2011, **133**, 1176.
35 K. E. Knowles, H. D. Nelson, T. B. Kilburn and D. R. Gamelin, *J. Am. Chem. Soc.*, 2015, **137**, 13138.
36 W. D. Rice, H. McDaniel, V. I. Klimov and S. A. Crooker, *J. Phys. Chem. Lett.*, 2014, **5**, 4105.
37 S. Liu, H. Zhang, Y. Qiao and X. Su, *RSC Adv.*, 2012, **2**, 819.
38 F. Bensebaa, C. Durand, A. Aouadou, L. Scoles, X. Du, D. Wang and Y. L. Page, *J. Nanopart. Res.*, 2010, **12**, 1897.
39 Y. Chen, S. Li, L. Huang and D. Pan, *Inorg. Chem.*, 2013, **52**, 7819.
40 W. Xiong, G. Yang, X. Wu and J. Zhu, *ACS Appl. Mater. Interfaces*, 2013, **5**, 8210.
41 J. I. Pankove, *Optical Processes in Semiconductors*, Dover Publication, New York, 1971.
42 T. Ogawa, T. Kuzuya, Y. Hamanaka and K. Sumiyama, *J. Mater. Chem.*, 2010, **20**, 2226.
43 Y. Hamanaka, T. Ogawa and M. Tsuzuki, *J. Phys. Chem. C*, 2011, **115**, 1786.